EUROFUSION WPJET1-CP(16) 15020

D Van Eester et al.

Recent ion cyclotron resonance heating experiments in JET in preparation of a DT campaign

Preprint of Paper to be submitted for publication in
Proceedings of 26th IAEA Fusion Energy Conference

This work has been carried out within the framework of the EUROfusion Consortium and has received funding from the Euratom research and training programme 2014-2018 under grant agreement No 633053. The views and opinions expressed herein do not necessarily reflect those of the European Commission.

Recent ion cyclotron resonance heating experiments in JET in preparation of a DT campaign

D. Van Eester[1], E. Lerche[1,2], Y. Kazakov[1], P. Jacquet[2], V. Bobkov[3], K. Crombé[1,4], A. Czarnecka[5], R. Dumont[6], J. Eriksson[7], L. Giacomelli[8], C. Giroud[2], M. Goniche[6], C. Hellesen[7], V. Kiptily[2], T. Koskela[9], M. Nocente[10], M. Santala[2,11], M. Schneider[6], H. Weisen[12] and JET contributors[*]

[1]LPP-ERM/KMS, EUROfusion Consortium Member, TEC, Brussels, Belgium
[2]CCFE, Culham Science Centre, Abingdon, OX14 3DB, UK
[3]Max-Planck-Institut für Plasmaphysik, Garching, Germany
[4]Department of Applied Physics, Ghent University, Ghent, Belgium
[5]Institute of Plasma Physics and Laser Microfusion, Hery 23, Warsaw, Poland
[6]CEA, IRFM, F-13108 Saint-Paul-lez-Durance, France
[7]Department of Physics and Astronomy, Uppsala University, Uppsala, Sweden
[8]Istituto di Fisica del Plasma "Piero Caldirola", IFP-CNR, Milano, Italy
[9]NERSC, MS 59R4010A Berkeley, CA 94720, USA
[10]Dipartimento di Fisica "G. Occhialini", Università di Milano-Bicocca, Milano, Italy
[11]VTT Technical Research Centre, FI-02044 Espoo, Finland
[12]Ecole Polytechnique Fédérale de Lausanne, SPC, CH-1015 Lausanne, Switzerland
[*]See the author list of "Overview of the JET results in support to ITER" by X. Litaudon et al. to be published in Nuclear Fusion special issue: "Overview and summary reports from the 26th Fusion Energy Conference (Kyoto, Japan, 17-22 October 2016)"

Corresponding Author: d.van.eester@fz-juelich.de

Abstract:
Since 2011 JET is equipped with a Beryllium "ITER-like" wall (ILW) and a Tungsten divertor [1]. As it can lead to reduced core temperature and even radiative collapse, high Z core impurity accumulation has to be avoided. Hydrogen minority ion cyclotron heating at sufficiently high power ($> 4MW$ in JET) is already well known to be an effective cure for this problem [2, 3, 4, 5, 6, 7]. In the context of exploring the available options for a $D-T$ campaign but without actually using T, this paper reports on investigations checking if D majority ion cyclotron resonance heating (ICRH) scenarios exist that can simultaneously ensure a high ion heating efficiency - needed for reaching fusion relevant temperatures - *and* impurity chase-out.

1 Introduction

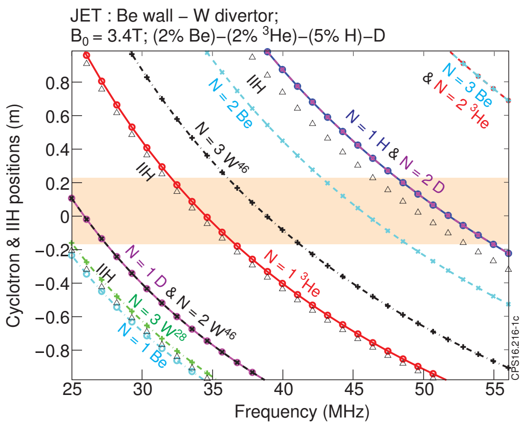

FIG. 1: Cyclotron and ion-ion hybrid (triangles) layers in JET as function of the ICRH frequency for a $(5\%H)-(2\%^3He)-(2\%Be)-D$ *plasma; N is the cyclotron harmonic.*

A key challenge in metal wall tokamaks and in particular in JET remains the fact that one simultaneously needs to keep the heat load on the divertor manageable while ensuring the plasma core is not contaminated by high Z material so that fusion relevant temperatures can be reached. Whereas W is chosen purposely for the divertor to withstand the high heat loads, penetration of minute amounts of Tungsten into the main plasma enhances the radiation and hence e.g. the risk for disruptions triggered by a thermal quench. Nowadays, strike point sweeping is routinely used at JET to spread the heat load over a bigger area of the divertor. Already in the 90's, it was demonstrated in TEXTOR that Tungsten could be chased successfully out of the plasma by applying ICRH at a sufficient power level [8]. An immediate question then comes to mind: Can such chase-out also be guaranteed for scenarios aiming at bulk ion heating which maximise the neutron rate from $D-T$ fusion reactions? Recent JET experiments have been done to start answering that question, but without actually using T to avoid excessive neutron production. To give an idea of the options, the positions of the cyclotron layers and ion-ion hybrid (mode conversion) layers for a D plasma typical for JET and fixing the magnetic field at $B_o = 3.4$ are depicted in Fig. 1. It is readily seen that 2 minority scenario's can be explored: (i) minority H heating and/or $N = 2$ D heating at $f = 51MHz$ and (ii) minority ^3He heating at $f = 33MHz$. A third scenario was equally tested: (iii) simultaneous H & ^3He minority heating by combined use of these 2 RF frequencies.

2 Experimental results

The reference plasma adopted had the following parameters: Central density and temperature were $N_o \approx 6-7\times10^{19}m^{-3}$ and $T_o \approx 6keV$, respectively. Long, stabilized sawteeth were observed in discharges where fast particles were created by the applied radio frequency (RF) heating. As a result, the central temperature was flattened inside the $q = 1$ surface (with minor radius of $\approx 0.2m$) and fell by as much as $1-2keV$ during a sawtooth crash, but subsequently recovered. The magnitude of the magnetic field at the geometric axis was $B_o = 3.4T$; the total plasma current was $I_p = 2MA$. Up to 7MW of RF power and 15MW of beam power were coupled, resulting in a stored energy level of $4MJ$. The H98 confinement factor was close to 1 in the H minority pulses in which RF and NBI were applied simultaneously; it was lower in the ^3He pulses.

Figure 2 depicts how the central ion and electron temperature change as a function of the applied RF power. As anticipated from theory, the H minority heating scenario gives rise to the highest electron temperatures ($T_{e,o} \approx 6.3keV$) since highly energetic tails are formed which slow down on electrons. Adding $4MW$ of RF power to $15MW$ of NBI power increases $T_{e,o}$ by almost $0.5keV/MW$. The most modest electron temperature is obtained when relying on ^3He minority heating. The increase of the electron temperature as a function of the applied RF power is similar, however. For that scenario, the ion temperature is about $5.5keV$ and hardly varies as a function of the wave power. The performance of the mixed frequency scheme lies in between that relying on 2 separate frequencies when looking at the electron temperature (increase per MW again similar) but is the best of all 3 schemes for ensuring ion heating. Ion temperatures up to $6.4keV$ were obtained.

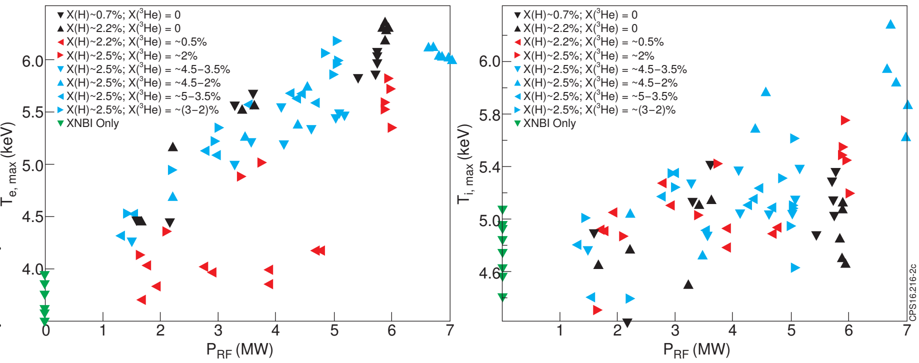

FIG. 2: Core electron and ion temperatures as a function of the RF power for the 3 types of shots. The H and ^3He concentrations are the estimates based on the light in the divertor; the concentrations at the location where the wave absorption occurs may be different.

Case (i): Clear signs of the creation of a fast D tail where seen when no H was puffed into the machine ($X[H] < 1\%$): The count rates of the neutral particle analyser in bins of a few hundred keV reached its highest levels when both (D) neutral beam injection and RF power were at the maximum requested power (not shown). The time-of-flight neutron detector allows to analyse the D fast particle population on the basis of info collected from neutrons coming from the $D-D$ reaction. Figure 3 shows the neutron spectra and corresponding fits for the shot in which D second harmonic heating is significant, and the shot for which the H minority heating is dominating. As the detector is based on a time-of-flight principle, fast particles are on the left of the plot while thermal particles are on the right. The contribution from the beam distribution is clearly visible. It is almost identical in both shots; a NBI-only reference was added to allow a clear identification. The changes of the neutron spectrum brought about by RF heating are much larger than for different NBI-only scenarios. The RF induced fast ion tail on the other hand is clearly noticeable at low $X[H] \approx 0.5\%$ while it is much less pronounced when H minority heating dominates ($X[H] \approx 2.5\%$). Deuterium tail data from the high energy neutral particle analyser confirm this result: The fast particle flux is an order of magnitude higher when no H is injected in the plasma. Sawtooth stabilisation ensured no sawteeth to be seen at all in the high power phase of the shot. When puffing H gas and increasing its concentration to $X[H] \approx 3\%$, long sawteeth ($\tau_{ST} \approx 0.5s$) were seen. The electron temperature is a few hundred eV higher in presence of efficient H minority heating and the confinement is marginally improved while Be impurity levels are essentially untouched. While the density is similar and the ion temperature is marginally lower throughout, the electron temperature differs in the centre because of the different sawtoothing behaviour. The total neutron rate confirms the existence of a fast D subpopulation: Without injecting H but applying ICRH, the observed neutron rate is about $4.2 \times 10^{15} n/s$ while it drops to

$3.2 \times 10^{15} n/s$ when a few percent of H is added. In absence of RF power but at a similar NBI power level (10% lower), the rate further drops to $1.8 \times 10^{15} n/s$, underlining the role of RF heating.

Case (ii): Adopting $f = 33MHz$ and puffing modest amounts of ^3He into the machine, the potential of $N = 1$ ^3He heating was studied. Sawteeth are gradually better stabilised when the ^3He concentration is increased, reflecting the ^3He absorption becoming more efficient. Concentrations below 1% yield poor electron heating and sawtoothing periods of the order of $250ms$ while for $X[^3He] \approx 3\%$ sawteeth have been further stabilised, their period being of the order of $1s$. In spite of the fact that no RF power is thought to directly reach the D majority, the minority ion heating has consequences for the majority population. The ion temperature is $500eV$ higher which in turn results in an increase by 50% of the neutron rate. The H98 confinement factor which is of order 1 for H minority shots, drops to 0.7 at low $X[^3He]$ and partly recovers, reaching a value of 0.95 when $X[^3He] \approx 3\%$. The change in sawtooth behaviour allows to reach core temperatures up to $2keV$ higher. The improved heating performance reduces the influx of impurities and yields a higher stored energy. Evidence of a modest tail is observed by the neutral particle analyser. As the highest ^3He concentration reached was a factor of 2 under what is thought to be the optimal value, it is believed that improvement of this heating scheme is still possible.

Case (iii): While the highest electron temperatures were reached in the minority H regime, the highest *ion* temperatures were achieved combining the 2 minority heating schemes. Temperatures of the order of $6keV$ were reached both for ions and electrons. At sufficient power and at the highest minority concentrations explored, sawtooth stabilisation was observed in all 3 schemes. The best confinement is obtained for H minority heating while the worst is obtained for ^3He minority heating. The 2-frequency operation was only crudely explored and should be re-addressed in later experiments. Scanning concentrations and densities over a wider range, and exploring the impact of the optimal choice of magnetic field and phasing would be beneficial.

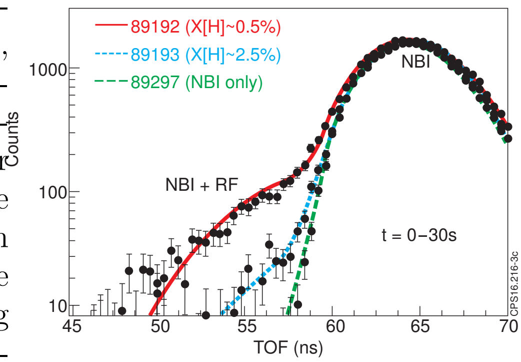

FIG. 3: D population signature from the time-of-flight neutron detector highlighting the difference between the D fast ion population in presence (#89193) and absence (#89192) of strong H minority heating.

3 Fast ion dynamics and ICRH-NBI synergy

The lost ion diagnostic detects RF induced highly energetic ions that escape from the main plasma. It allows to determine the particle's energy and pitch angle, which helps understanding the auxiliary heating performance [9]. Assuming Coulomb collisions are too infrequent to be accounted for allows to trace back the orbit of energetic ions to the location where they got accelerated.

Case (i): Figure 4 shows the lost ions observed when adopting the hydrogen minority heating scheme ($51MHz$). Lost ions in the MeV range are detected irrespective of whether or not additional H is puffed in the machine; the red line in the plot locates the non-Doppler shifted cyclotron layer. Higher energy particles are observed when the conditions for efficient H heating are satisfied, but a broader pitch angle scattering is observed when the H concentration is low. Consistent with the stabilising effect brought about by a fast ion population, the electron temperature exhibits monster sawteeth in these shots [10].

As the ILW is made of Beryllium and interaction of the plasma with the wall is unavoidable, concentrations of the order of 1% of Be are thought to be present in JET. Various nuclear reactions exist that involve Be. Gamma ray emission is often a byproduct of such reactions. Studying the gamma ray emission adds insight on the fast ion populations present in the discharges. Gammas from the nuclear reaction $^{9}Be(p,\gamma)^{10}B$ have been identified in the gamma spectrum [11]. As protons with energies exceeding 700keV are required for this reaction, this identifies part of the lost ions observed as RF accelerated fast Hydrogen. Traces of gamma rays from the reactions $^{9}Be(D,n\gamma)^{10}B$ and $^{12}C(D,p\gamma)^{13}C$ have equally been observed, demonstrating the presence of Deuterons with energies exceeding 500keV. Neutron diagnostics equally reveal the presence of fast Deuterons. When no H is added to the discharge the highest neutron rate is reached.Consistent with minority heating, the H minority heating shot with $X[H] \approx 3\%$ exhibits *lower* D energies.

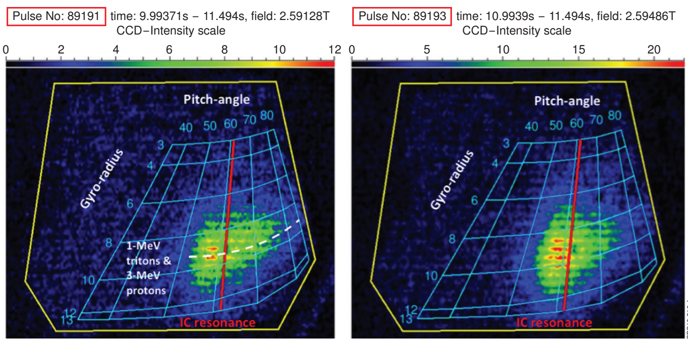

FIG. 4: Fast ion losses detected when using $f = 51MHz$; the left subplot shows the losses when no additional H was puffed ($X[H] \approx 0.5\%$) and the right subplot shows the equivalent result when $X[H] \approx 3\%$.

Case (ii): When adopting $f = 33MHz$, sawtooth stabilisation is observed even at very low levels of ^{3}He. From the lost ion detector one deduces that at low $X[^{3}He]$, the major radius position at which most high energy particles are created moves from the high to the low field side of the ^{3}He (cold ion cyclotron) resonance when the RF power increases, consistent with the fraction of the perpendicular to the total energy increasing with RF power and the banana tips receding towards the low field side. The opposite trend is observed when increasing the minority concentration: The maximum is found further to the high field side at higher $X[^{3}He]$. Recall that the maximum absorption does not coincide with the cold plasma resonance but with the location at which the optimal wave polarisation to ensure good heating is reached.

The experimentally used ^{3}He concentration is an estimate, deduced from the relative light from the He and H isotopes in the divertor. Its value is likely not to be constant inside the vessel. As the ion-ion hybrid (IIH) resonance position critically depends on the plasma composition, and provided the major radius corresponding to the maximum of the lost ion population crudely indicates where the IIH resonance lies, this yields an independent guess of $X[^{3}He]$. Such a cross-check suggests that in order to be consistent with the experimental findings, the $X[^3He]$ estimate based on the divertor light should be corrected by a "core peaking" factor of $1.5 - 2$. A similar correction was found in the past (see e.g. [12]).

Case (iii): The dual frequency shot in which the ^3He ions were most energetic was also the shot in which the highest bulk ion temperature ($6.2keV$) as well as neutron rate ($4 \times 10^{15}/s$) were observed. The peak neutron rate is believed to be the result of the combined heating schemes, $N = 1$ ^3He minority heating allowing to increase the temperature of one of the fuel ions of the $D -^3 He$ reaction (35kW of fusion power was generated from that reaction in that shot) while Coulomb collisionally raising the temperature of the bulk D ions. The latter are heated by waves launched with $f = 51MHz$, which also boost the energy of the beam ions to increase the $D - D$ fusion rate.

4 High Z populations chase-out

The concentration of Tungsten is determined from soft x-ray and VUV radiation measurements, taking into account the local electron density and temperature [14]. Figure 5 summarises the obtained results for the 3 heating schemes. To the exception of the high $X[W]$ dots at $\approx 8 \times 10^{-4}$ in the left subfigure, the core Tungsten concentrations are of order $X[W] \approx 3 - 4 \times 10^{-4}$. The high $X[W]$ dots underline that impurity removal necessitates a sufficient amount of RF power effectively coupled to the core plasma as they correspond to $X[^3He]$ below 1%, too low for minority heating to be efficient. The lowest Tungsten concentrations were obtained adopting the 2-frequency heating scheme (triangles). Apart from the deviating evidence at too low $X[^3He]$, the separate H minority and ^3He heating scenarios show a similar dependence on the RF power level: strongly increasing with power in the outer layers of the plasma, weakly increasing at mid-radius and stagnating or possibly weakly decreasing at higher power levels in the core. The core concentration is markedly higher than that at the edge. Applying NBI power only (at the same level as used for the other experiments: $15MW$), the estimate W concentrations are 2.2×10^{-4}, 5.5×10^{-5} and 1.1×10^{-5}, respectively i.e. similar in the core but lower by a factor 2-3 away from it compared to values when both NBI and RF heating were applied. Baranov compared the peaking of the radiation profile in presence and absence of RF heating [13] and confirms that increasing the RF/NBI power fraction is beneficial for reducing the core radiation peaking. At the available power level, ICRH thus seems capable to prevent increased core contamination but it does so at the expense of widening the $X[W]$ profile. Analysis of the soft x-ray data, the total bulk radiated power and spectroscopic analysis of Ni light corroborates the relative performance of the 3 studied RF heating scenarios. While the 2D soft x-ray profile shows a monotonic dependence, the 2D radiation profile obtained from bolometry has a maximum at the core (contributing little to the overall radiation in view of the volume effect, though), going through a local minimum around mid-radius and increases towards the edge, the dominant contribution by far coming from the divertor. Although various hints point in the right direction, clear evidence that a sufficient level of RF power curtails the diffusion of high populations to the plasma core is - at this moment - *not* yet available for plasmas relying on ^3He heating.

Further tests to demonstrate this potential convincingly are highly desirable.

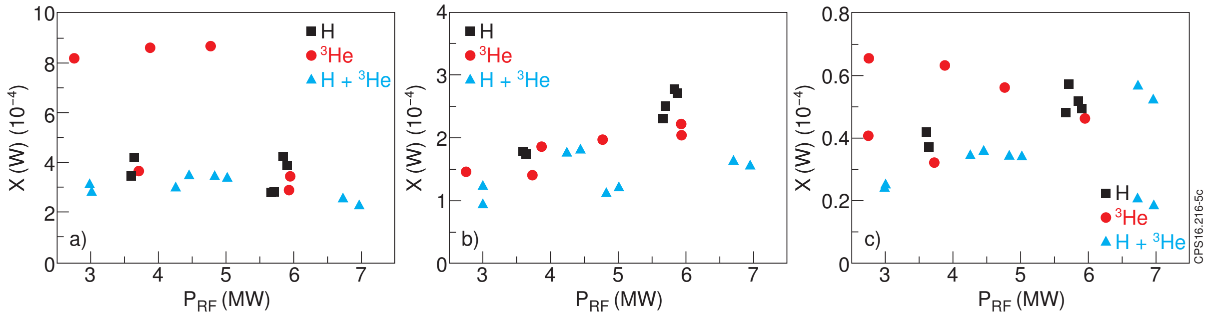

FIG. 5: Summary of the estimated Tungsten concentrations for the various heating schemes at 3 locations in the plasma: (a) $\rho/a_p = 0.0$, (b) $\rho/a_p = 0.45$, (c) $\rho/a_p = 0.70$.

5 Conclusions

Three scenarios for high magnetic field ($B_o = 3.4T$) operation were tested and compared: (i) Hydrogen minority heating, (ii) ^3He minority heating and (iii) the combination of the former 2 by simultaneous use of 2 RF frequencies. Whereas the former of these schemes has already proven to have potential, the second is to be preferred for application in $D-T$ plasmas since ^3He minorities can be used to increase the $D-T$ fusion reactivity and would then combine the role of majority ion heater via Coulomb slowing down with that of high Z impurity chaser. The third scenario was included as a back-up option in case the ^3He minority scheme would not perform its combined role well.

The best $D-T$ relevant results were obtained when combining the 2 minority heating schemes, although pure second harmonic D heating (no injected H) proved to be beneficial as well. This scheme becomes efficient at high density whereas earlier experiments (see e.g. [12]) typically were done at lower densities ($3-4\times10^{19}/m^3$ compared to the presently used $6\times10^{19}/m^3$). As expected from theory, operation aimed at heating a ^3He minority but performed in absence of ^3He yields the highest Tungsten contamination, no efficient core absorber being available.

Fast particle diagnostics detected high energy populations in conditions where they were theoretically expected for efficient H or ^3He minority heating. Some findings suggest the synergistic effects of RF and NBI heating play a role in some scenarios. In absence of minorities that efficiently absorb the power, D bulk or beam ions can assume the role of dominant absorber, an effect that can be exploited. Although plasma-wall interaction is avoided as much as possible, some of the Be from the wall finds its way to the plasma. Neutrons and gamma rays from nuclear reactions involving parasitic Be and one of the working gases (H, ^3He or D) yield interesting information on fast populations.

Similar core W concentrations were found for the various tested scenarios. Expectedly, operation at too low $X[^3He]$ yields a higher W concentration: Poor RF heating schemes necessitate bigger electric field amplitudes and typically give rise to enhanced plasma-wall interaction. So far, no firm conclusions can be drawn w.r.t. the ability to ensure high Z chase-out both since the adopted power level was marginal and since the explored minority concentration interval was too limited: Although theoretical models indicate that there is an optimal minority concentration, the reduction of the heating efficiency when going *beyond* the optimal concentration was never observed in the experimentally explored ^3He minority concentration range. The core Tungsten concentration scales with the RF power but the radiated power grows slower than the amount of power launched. Also other impurities were observed to be invading the plasma less when reaching better heating performance.

The present experiments constitute a rich pool for modellers.

6 Acknowledgements

This work has been carried out within the framework of the EUROfusion Consortium and has received funding from the Euratom research and training programme 2014-2018 under grant agreement No 633053. The views and opinions expressed herein do not necessarily reflect those of the European Commission.

References

[1] NEU, R., et al., Phys. Plasmas 20 (2013) 056111.

[2] GONICHE, M., et al., Proc. 41th EPS conf. on Contr. Fusion & Plasma Phys., Berlin, Germany, 45 (2014) O4.129.

[3] LERCHE, E., et al., "ICRH for core impurity mitigation in JET-ILW", WPJET1-PR(15)28, accepted for publication in Nuclear Fusion.

[4] LERCHE, E., et al., "ICRH for Mitigation of Core Impurity Accumulation in JET-ILW", Proc. 25th IAEA Fusion Energy Conference, St. Petersburg, Russia (2014) EX/P5-22.

[5] GIROUD, C., et al., "Progress in understanding of impurity transport at JET" (2006) Rep. EFDA-JET-CP(06)05-21.

[6] CARRARO, L., et al., "Impurity profile control in JET plasmas with RF power injection" (2007) Rep. EFDA-JET-CP(07)03/05.

[7] VALISA, M., et al., Proc. 49th Annual Meeting of the Division of Plasma Physics (2007) Orlando (USA).

[8] VAN OOST, G., et al., Proc. EPS Conf. (1995) Bournemouth, United Kingdom

[9] KIPTILY, V.G., et al., Nuclear Fusion 49 (2009) 065030

[10] GRAVES, J., et al., Plasma Physics and Controlled Fusion 47 12B (2005) B121-B133

[11] KIPTILY, V.G., et al. , Nuclear Fusion 42 (2002) 999

[12] VAN EESTER D., et al., Plasma Phys. Control. Fusion 54 (2012) 074009

[13] BARANOV, Y., et al., "Accumulation trend of heavy impurities in the core of Neutral Beam and ICRF heated plasmas in JET", submitted to *Plasma Phys. Contr. Fusion*

[14] PÜTTERICH, T., et al., Plasma Phys. Control. Fusion 55 (2013) 124036